Annals of Botany **115**: 211–226, 2015
doi:10.1093/aob/mcu235, available online at www.aob.oxfordjournals.org

ANNALS OF BOTANY
Founded 1887

Floral biology and ovule and seed ontogeny of *Nymphaea thermarum*, a water lily at the brink of extinction with potential as a model system for basal angiosperms

Rebecca A. Povilus[1,*,†], Juan M. Losada[1,2,†] and William E. Friedman[1,2]

[1]*Department of Organismic and Evolutionary Biology, Harvard University, 26 Oxford Street, Cambridge, MA 02138, USA and* [2]*Arnold Arboretum of Harvard University, 1300 Centre Street, Boston, MA 02131, USA*
** For correspondence. E-mail rpovilus@fas.harvard.edu*
[†]*These authors contributed equally to this work.*

Received: 23 July 2014 Returned for revision: 11 September 2014 Accepted: 21 October 2014 Published electronically: 14 December 2014

• **Background and Aims** *Nymphaea thermarum* is a member of the Nymphaeales, of one of the most ancient lineages of flowering plants. This species was only recently described and then declared extinct in the wild, so little is known about its reproductive biology. In general, the complete ontogeny of ovules and seeds is not well documented among species of *Nymphaea* and has never been studied in the subgenus *Brachyceras*, the clade to which *N. thermarum* belongs.
• **Methods** Flowers and fruits were processed for brightfield, epifluorescence and confocal microscopy. Flower morphology, with emphasis on the timing of male and female functions, was correlated with key developmental stages of the ovule and the female gametophyte. Development of the seed tissues and dynamics of polysaccharide reserves in the endosperm, perisperm and embryo were examined.
• **Key Results** Pollen release in *N. thermarum* starts before the flower opens. Cell walls of the micropylar nucellus show layering of callose and cellulose in a manner reminiscent of transfer cell wall patterning. Endosperm development is *ab initio* cellular, with micropylar and chalazal domains that embark on distinct developmental trajectories. The surrounding maternal perisperm occupies the majority of seed volume and accumulates starch centrifugally. In mature seeds, a minute but fully developed embryo is surrounded by a single, persistent layer of endosperm.
• **Conclusions** Early male and female function indicate that *N. thermarum* is predisposed towards self-pollination, a phenomenon that is likely to have evolved multiple times within *Nymphaea*. While formation of distinct micropylar and chalazal developmental domains in the endosperm, along with a copious perisperm, characterize the seeds of most members of the Nymphaeales, seed ontogenies vary between and among the constituent families. Floral biology, life history traits and small genome size make *N. thermarum* uniquely promising as an early-diverging angiosperm model system for genetic and molecular studies.

Key words: Early-diverging angiosperm, embryo, endosperm, evo-devo, female gametophyte, flower biology, megagametogenesis, megasporogenesis, *Nymphaea thermarum*, Nymphaeales, perisperm, protogyny, seed development, stigma.

INTRODUCTION

Nymphaea thermarum, a member of one of the most ancient lineages of flowering plants, is a remarkable species from many perspectives. This annual, miniature water lily was originally described from a restricted hot-spring habitat in Rwanda (Fischer, 1988) and was recently declared as extinct in the wild (Fischer and Magdalena-Rodriguez, 2010). With little known about its physiology or reproductive biology, germplasm is currently maintained in just a few botanical collections worldwide. We propose that, far from being written off as a botanical curiosity and evolutionary dead end, *N. thermarum* is uniquely poised to help unravel many long-standing questions about the origin and early evolution of angiosperms, the clade that includes the majority of land plant diversity.

Early-diverging angiosperm lineages are particularly poor in species amenable to genetic experimentation. Most taxa are woody and perennial (e.g. *Amborella*, Austrobaileyales, Chloranthales and the vast majority of magnoliids), and even the aquatic and typically perennial life history of most members of Nymphaeales make them difficult to maintain in large numbers in a controlled environment. *Nymphaea thermarum*, while aquatic, requires only shallow water, has a relatively short generation time of 5–6 months and is small enough that hundreds of individuals can be grown in a single greenhouse room. Like *Arabidopsis thaliana*, *N. thermarum* self-fertilizes, is also capable of outcrossing and reproduces prolifically by seed. Finally, *N. thermarum* has a genome size that is on a par with other established flowering plant model systems (roughly twice as large as the genome of *A. thaliana*) (Pellicer *et al.*, 2013). Any attempt to develop this species into a model system, including creation of isogenic lines and development of stable transformation protocols, would benefit from a detailed knowledge of its reproductive biology. In addition, such information will be invaluable for conservation efforts, such as propagation and

maintenance of remaining genetic diversity, with the potential to reintroduce this species into its native habitats.

Nymphaeales is one of the most ancient angiosperm lineages, either sister to all flowering plants except *Amborella* or sister to *Amborella* and together forming the sister group to all other flowering plants (Maia *et al*., 2014; Ruhfel *et al*., 2014). While all members of Nymphaeales are aquatic, there has nonetheless been considerable evolutionary diversification over the nearly 125 million years of history documented in the fossil record (Qiu *et al*., 1999; Friis *et al*., 2001, 2006, 2011; Magallón *et al*., 2013; Doyle and Endress, 2014; Iles *et al*., 2014). Recent molecular dating studies corroborate the ancient age of Nymphaeales, with Hydatellaceae diverging from its sister group Nymphaeaceae plus Cabombaceae roughly 127 million years ago (Saarela *et al*., 2007; Iles *et al*., 2014). Thus, studies within the clade present a unique opportunity to examine how reproductive characters have diversified in these aquatic plants since the Early Cretaceous.

Fortunately, the historical popularity of *Nymphaea* flowers for ornamental and cultural uses means that the macroscopic (morphological) aspects of reproductive biology have been documented for many taxa (Moseley, 1961; Wiersema, 1988 and references therein; Endress, 2010). Protogyny (female receptivity occurring before shedding of pollen within the same flower) is the norm in *Nymphaea* flowers (Schneider and Chaney, 1981; Schneider, 1982; Capperino and Schneider, 1985; Williams *et al*., 2010), as is true of the vast majority of hermaphroditic basal angiosperms. For *Nymphaea*, the separate female and male phases are punctuated by floral movements: the flower opens one day or evening as functionally female, closes, and reopens as functionally male. Intriguingly, many of the exceptions to protogyny that have been documented among basal angiosperm lineages with hermaphroditic flowers involve taxa within *Nymphaea* (Endress, 2010). *Nymphaea thermarum* is a member of the *Brachyceras* subgenus (Borsch *et al*., 2011), a pan-tropical clade often referred to as the tropical day-blooming water lilies, while the several other subgenera in *Nymphaea* are circumscribed according to biogeography and whether flowering is nocturnal or diurnal. There are ∼46 extant species in *Nymphaea*, making it the largest genus in Nymphaeaceae, which, with 58 species, is by far the largest family within Nymphaeales, compared with ten species in Hydatellaceae and six in Cabombaceae (Stevens, 2001).

The developmental morphology of flowers and fruits within Nymphaeales has been documented in most genera and subgenera (Chiflot, 1902; Heslop-Harrison, 1955*a*, *b*; Moseley, 1961; Khanna, 1964*b*; Ramji and Padmanabhan, 1965; Schneider, 1976, 1982, 1983; Schneider and Moore, 1977; Schneider and Chaney, 1981; Moseley *et al*., 1984; Williamson and Moseley, 1989; Schneider *et al*., 2003; Endress, 2001, 2005; Grob *et al*., 2006; Rudall *et al*., 2007; Zhou and Fu, 2007; Hu *et al*., 2009; Rudall *et al*., 2009; Sokoloff *et al*., 2009, 2010; Vialette-Guiraud *et al*., 2011). Features of female gametophyte development, fertilization and seed development have also been studied, but are scattered across a century of embryological literature (Cook, 1902, 1906, 1909; Conard, 1905; Seaton, 1908; Martin, 1946; Meyer, 1960; Khanna, 1964*a*, *b*, 1965, 1967; Valtzeva and Savich, 1965; Schneider, 1978; Schneider and Ford, 1978; Batygina *et al*., 1980, 1982; Schneider and Jeter, 1982; Winter and Shamrov, 1991; Van Miegroet and Dujardin, 1992; Orban and Bouharmont, 1998; Bonilla-Barbosa *et al*., 2000; Floyd and Friedman, 2000, 2001; Yamada *et al*., 2001; Williams and Friedman, 2002; Baskin and Baskin, 2007; Friedman, 2008; Zhou and Fu, 2008; Rudall *et al*., 2008, 2009; Friedman *et al*., 2012). An integrative approach to the ontogenies of the gametophyte, embryo, endosperm and perisperm in *Nymphaea thermarum* will fill a conspicuous gap in our knowledge of ovule and seed development within Nymphaeales.

In this study we document the reproductive development of *N. thermarum* from floral bud emergence through fertilization and seed development to germination. The goals are to correlate the timing of key events during floral and ovule development with pollination and seed development in order to provide an integrated view of the reproductive biology of *N. thermarum*. This, we hope, can be used as a reference for future experimental and genetic work and/or conservation efforts. In addition, we seek to document in detail the ontogeny and nutritional status of the endosperm, embryo and maternal tissues during seed development. In turn, these embryological features of *N. thermarum* are used to examine the evolutionary-developmental history of a suite of reproductive characters within the broader comparative context of the Nymphaeales. As will be seen, heterochronic alterations in floral development have been an important force in the evolutionary history of the clade and specifically in the origin of a set of apomorphic features in *N. thermarum*.

MATERIALS AND METHODS

Plant material

Nymphaea thermarum seeds from the Botanische Gärten der Universität Bonn (Bonn, Germany) were sown and plants grown at the greenhouses of the Arnold Arboretum of Harvard University, according to the guidelines of Fischer and Magdalena-Rodriguez (2010). To study female gametophyte development, flowers were collected at different developmental stages from flower bud to flower opening. Flowers were measured over the 12 days between floral bud emergence and the first day of anthesis in order to generate a correlation between bud length and number of days until anthesis. To evaluate seed development, self-fertilized flowers and fruits were collected at daily intervals after first flower opening until seed set and release. Seeds were allowed to germinate in a Petri dish filled with water, kept at room temperature and collected at regular intervals until the emergence of the first leaf. Collected material was fixed in 4 % v/v acrolein (Polysciences, New Orleans, LA, USA) in 1× PIPES buffer (50 mM PIPES, 1 mM $MgSO_4$, 5 mM EGTA), pH 6·8, for 24 h. Fixed material was then rinsed three times (1 h each time) with 1× PIPES buffer, dehydrated through a graded ethanol series and stored in 70 % ethanol.

Microscopy

Samples for sectioning were dehydrated though a graded ethanol series up to 100 % ethanol, then infiltrated with and embedded in glycol methacrylate (JB-4 Embedding Kit, Electron Microscopy Sciences, Hatfield, PA, USA). Embedded materials were serially sectioned in 4-μm thick ribbons with a Leica

RM2155 rotary microtome and mounted onto slides. Sections were stained with periodic acid–Schiff (PAS) reagent for insoluble polysaccharides (Feder and O'Brien, 1968) and counterstained with toluidine blue for general tissue structure (Feder and O'Brien, 1968). To detect the β-glucan callose, 0·1 % aniline blue in 0·1 N K_3PO_4 (Currier, 1957) was used. To visualize cellulose and other polysaccharides in cell walls, slides were stained with an aqueous solution of 0·07 % calcofluor white (Hughes and McCully, 1975).

Bright-field and differential interference contrast images were recorded with a Zeiss Axio Imager Z2 microscope equipped with a Zeiss HR Axiocam digital camera (Zeiss, Oberkochen, Germany). Imaging of callose was done with a Zeiss Axiophot microscope with epifluorescence (HBO 100) connected to an MRC Axiocam Zeiss digital camera and a cube filter with 365 nm excitation and 465 nm long-pass barrier emission wavelengths. Calcofluor-stained sections were imaged on a Zeiss LSM700 confocal microscope equipped with an AxioCam HRc camera (Zeiss, Oberkochen, Germany) with excitation at 405 nm and emission detection at 465 nm wavelengths.

Whole-mount samples for confocal microscopy were dissected to <2 mm in any dimension. Samples were rehydrated though a graded ethanol series to 100 % aqueous and stained for the Feulgen reaction according to Barrell and Grossniklaus (2005), with incubation times adjusted for size of the samples. Samples were then dehydrated in a graded ethanol series to 100 % ethanol. In the case of pre-fertilization and early post-fertilization ovules, samples were cleared by graded infiltration with Immersol 518f (Zeiss, Oberkochen, Germany). For older fertilized ovules and seeds, samples were infiltrated with and embedded in JB-4 glycol methacrylate (Electron Microscopy Sciences, Hatfield, PA, USA). Blocks were cut by hand with razor blades to remove superfluous tissue layers. Samples were mounted in a drop of Immersol 518f on custom well slides and imaged with a Zeiss LSM700 confocal microscope equipped with an AxioCam HRc camera. A two-pass, three-channel acquisition mode was used to maximize histochemical information: pass 1, excitation at 405 and 488 nm, emission detection between 400 and 520 nm (channel 1) and between 520 and 700 nm (channel 2); pass 2, excitation at 638 nm, emission detection between 520 and 700 nm (channel 3).

Digital image processing

Pictures, line drawings and figures were processed using either Image J (http://rsbweb.nih.gov/ij/index.html) or Adobe Creative Suite 5 (Adobe Systems, San Jose, CA, USA). For light microscopy, image manipulations were restricted to operations that were applied to the entire image. For confocal z-stacks, loss of signal with tissue depth was compensated for by using the Stack Contrast Adjustment Plugin for ImageJ (Čapek *et al*., 2006). In the cases where uneven thickness of overlying tissue resulted in uneven signal brightness within an optical section, channels were adjusted manually to compensate, resulting in even signal levels across an optical section.

Maximum projections of confocal z-stacks were generated in ImageJ using the 3D-Project tool. Three-dimensional surface models were created with the 3D-Viewer plugin in ImageJ, using the Surface setting on z-stacks in which each zone of interest had been manually outlined from each optical slice.

RESULTS

Floral and ovule morphogenesis

Flowers of *Nymphaea thermarum* are hermaphroditic (Fig. 1). Floral buds emerge from the ground-level shoot apical meristem ~12 d before anthesis. At this stage, the outermost tepals are green and the immature inner tepals have a white/cream coloration. Two ranks of anthers surround 6–11 separate carpels. Stigmatic surfaces are delimited by upturned carpel tips and are oriented towards the ventral side of the gynoecium. Carpels are characterized by parietal placentation with numerous ovule primordia per carpel (data not shown). Six days before anthesis, anthers develop a light yellow coloration, carpel walls begin to fuse, and their tips reflex. Ovules enlarge, with both integuments present, and the inner integument extends beyond the outer. Two days before flower opening, anthers increase in yellow pigmentation and papillate stigmatic surfaces are completely exposed. Ovule growth continues and an endostomic micropyle is formed.

One day before flower opening, the outer rank of anthers dehisces and stigmatic fluid is secreted from the suture of each carpel. On the first day of anthesis, flowers usually open in the morning and copious stigmatic fluid is present on the surface of the gynoecium. Ovules are mature, and are anatropous, bitegmic and crassinucellate. Flowers close in the afternoon. On the second morning of anthesis, flowers reopen and the remaining anthers dehisce to release loosely aggregated pollen, while the stigmatic surface is dry and discoloured. Fertilized ovules show a dramatic increase in size and starch content. Flowers re-close typically in the afternoon of the second day. Flowers may open for one or more additional days with continued pollen release. After that, the pedicel curls to draw the closed flower down to the soil level, often partially burying the developing fruit.

Female gametophyte development

The megaspore mother cell is distinguished from other cells of the nucellus by its larger size, large nucleus and prominent starch grains (Fig. 2A). Concurrently with micropyle formation, the first meiotic division occurs at the micropylar end of the megaspore mother cell (Fig. 2B). A tetrad of megaspores is formed at the completion of meiosis. (Fig. 2C). The three micropylar-most megaspores degenerate, while the chalazal-most megaspore persists and features a centrally positioned nucleus surrounded by starch grains (Fig. 2D). The first mitosis of the functional megaspore produces two nuclei surrounded by a mass of cytoplasm and starch (Fig. 2E). By this time, the nucellar tissue between the female gametophyte and the nucellar epidermis has degenerated or been crushed by expansion of the female gametophyte, leaving the female gametophyte in direct contact with the thickened walls of the nucellar epidermis. The female gametophyte then undergoes a second round of mitosis and cellularizes into three starch-filled small cells at the micropylar end (egg apparatus) and a larger starchless cell that occupies the rest of the female gametophyte (Fig. 2F). The mature

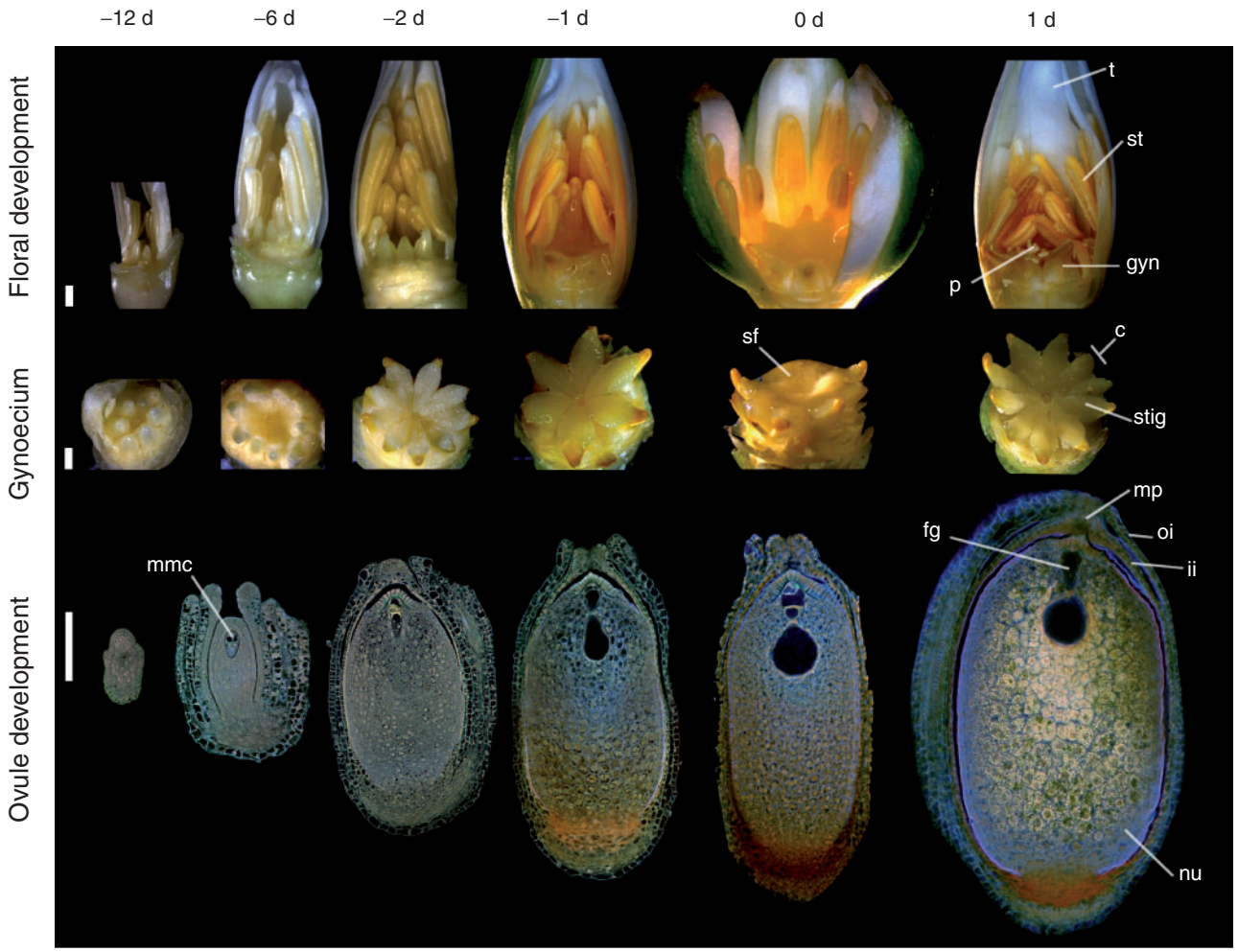

FIG. 1. Flower and ovule morphogenesis in *Nymphaea thermarum*. Stages in floral biology, gynoecium development and ovule morphogenesis are depicted at 12, 6, 2 and 1 days before anthesis, as well as the first and second day of anthesis (noted as -12 d, -6 d, -2 d, -1 d, 0 d and 1 d, respectively). Stereomicroscope images of floral buds (first row, some perianth removed to show all floral organs) and gynoecia (second row, all other floral organs removed), along with confocal optical sections of *N. thermarum* ovules pretreated for the Feulgen reaction and cleared (third row, whole ovules). (First row) Outer ranks of anthers dehisce and some stigmatic fluid is secreted at -1 d. Flowers then open for 2 consecutive days (0 d, 1 d), with a prominent drop of stigmatic fluid present at 0 d and fully dehisced anthers evident at 1 d. (Second row) Carpels begin to fuse at -6 d and the stigmatic surface is revealed by -2 d. Stigmatic fluid is present at -1 d and prominent at 0 d. (Third row) An endostomic micropyle is formed by -2 d. The mature female gametophyte, with an hour-glass shape, is present at -1 d. By 1 d, starch accumulation in nucellus (perisperm) is apparent. Abbreviations: c , carpel; fg, female gametophyte; gyn, gynoecium; ii, inner integument; mmc, megaspore mother cell; mp, micropyle; nu, nucellus (perisperm); oi, outer integument; p, pollen; sf, stigmatic fluid; st, stamen; stig, stigma; t, tepal. Scale bars = 100 μm.

egg apparatus consists of two synergids and one egg cell at the micropylar end. The large central cell nucleus resides at a circumferential constriction in the central cell, giving the female gametophyte an hour-glass shape (Fig. 2G). Prior to fertilization, the absence of nutrient reserves in the mature gametophyte contrasts with some starch accumulation in both the nucellus surrounding the chalazal end of the female gametophyte and in the micropylar nucellar epidermis.

Cells of the micropylar nucellar epidermis feature a highly elaborated inner face of the chalazal-most, periclinal wall, with discrete layers of cellulose and callose. The nucellar epidermis begins to form this distinct layer ∼6 d before anthesis (Fig. 3A). The inner periclinal walls, which contact or flank the developing female gametophyte, thicken and develop a convoluted appearance that persists through fertilization (Fig. 3B–D). This wall does not stain strongly with toluidine blue. Cellulose deposition coincides with elaboration of the inner periclinal wall 6 d before anthesis (Fig. 3E). Cellulose continues to accumulate up to anthesis (Fig. 3F–G). After fertilization, cellulose is absent from the site of pollen tube penetration (Fig. 3H, arrow). A discrete layer of callose is present on the micropylar-most face of this transfer cell-like wall ∼3 d before anthesis (Fig. 3J–K), but is conspicuously absent after fertilization (Fig. 3L).

Pollination, double fertilization and early endosperm differentiation

Prior to pollen deposition on the stigma surface, the subdermal tissue beneath the multicellular stigmatic papillae shows intense starch accumulation (Fig. 4A). These starch reserves

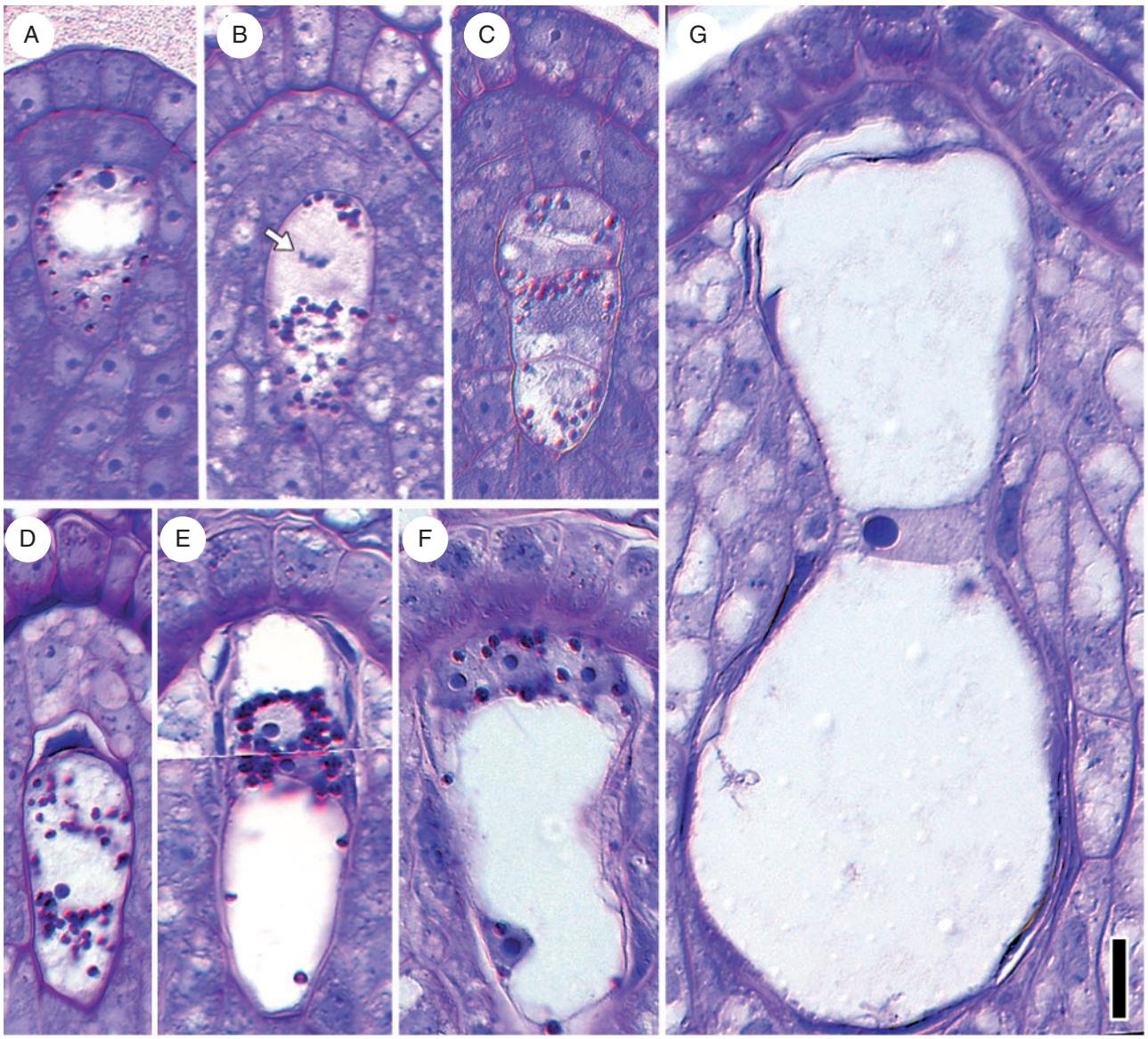

FIG. 2. Female gametophyte development in *Nymphaea thermarum*. Material was embedded in JB-4 resin, sectioned at 4 μm and stained with PAS reagent and toluidine blue. (A) Megaspore mother cell with starch granules (red/magenta) present in cytoplasm. (B) First meiotic division showing chromosomes (arrow) at the micropylar pole and starch granules at the chalazal pole. (C) Linear tetrad of four cellular megaspores. (D) Functional megaspore, formed from the chalazal-most megaspore, with degenerating micropylar megaspore. (E) Two-nucleate female gametophyte with starch surrounding the nuclei. This image represents a composite of two sequential sections. (F) Immature four-celled female gametophyte, with three cells at the micropylar end and one (the central cell) that occupies the rest of the female gametophyte. (G) Mature female gametophyte, devoid of starch and showing an hour-glass shape. Scale bar = 10 μm.

decrease dramatically upon pollen tube emergence from the pollen grains (Fig. 4B). Strikingly, pollen grains and pollen tubes also contain copious starch reserves through the time of fertilization. Starch presence in pollen grains may be related to pollination syndrome and/or metabolic activity (Baker and Baker, 1979), but significant quantities of starch in pollen tubes are rare among angiosperms. By the second day of anthesis, stigmatic cells are devoid of starch (Fig. 4C).

After entering the micropyle, the pollen tube penetrates the nucellar cap and female gametophyte. Two sperm cells are discharged into one of the synergids (Fig. 5A). Interestingly, at the time of sperm cell discharge the central cell nucleus is located next to the egg cell apparatus (Fig. 5B). This migration is temporary, and shortly after fertilization the central cell nucleus, now the primary endosperm nucleus, is located at its former position at the point of female gametophyte constriction.

On the first day of anthesis, the primary endosperm nucleus divides and a transverse wall is formed in the region of the central constriction of the former female gametophyte (Fig. 5B, C). Thus, two endosperm domains are created: a micropylar endosperm domain and a chalazal endosperm domain. Two nucleoli are present in the chalazal domain endosperm nucleus (Fig. 5B), but after migration to the chalazal-most end, a single nucleolus is present (Fig. 5C). The chalazal cell is cytoplasmically dense and develops a finger-like projection into the nucellus. Two days after anthesis, the two-celled embryo has

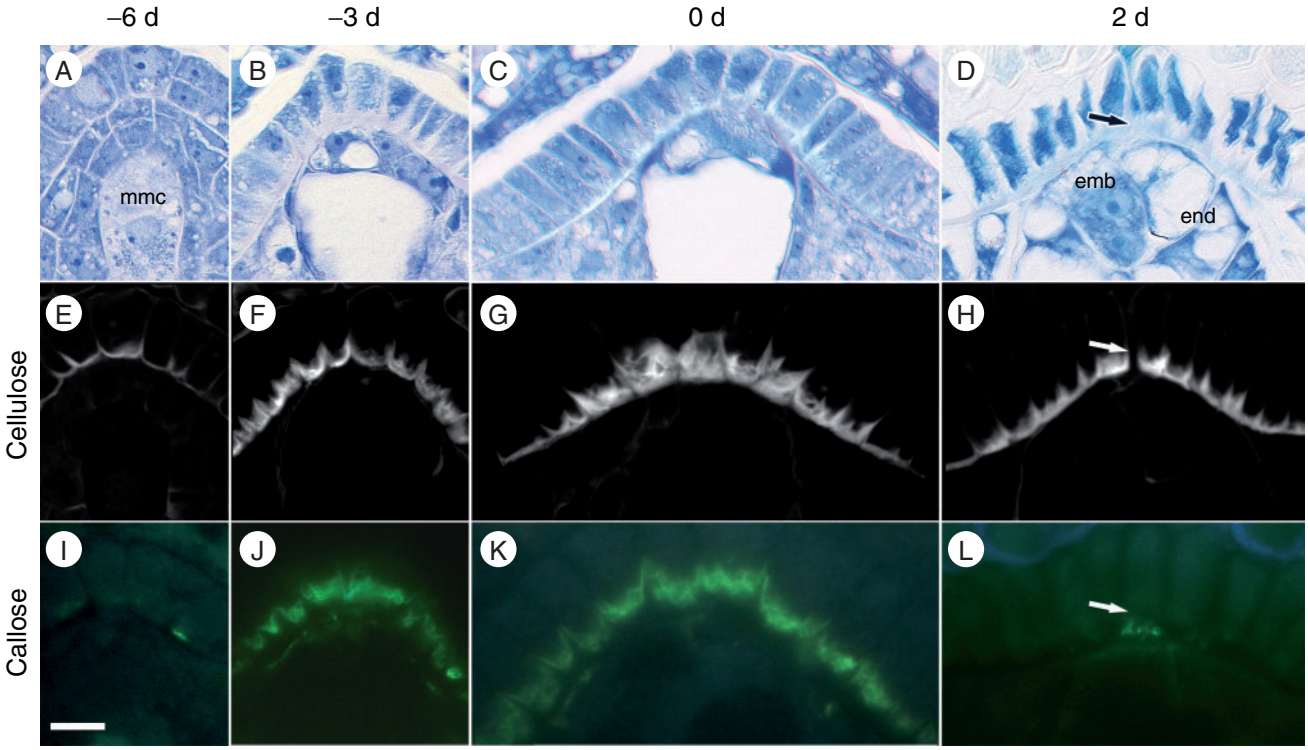

FIG. 3. Micropylar nucellar epidermis in *Nymphaea thermarum* developing ovules. Ovules from 6 days before anthesis (-6 d), megaspore mother cell stage (A, E, I); 3 days before anthesis (-3 d, immature four-celled female gametophyte stage; B, F, J), first day of anthesis (0 d, mature female gametophyte stage: C, G, K) and 2 days after anthesis (2 d, post-fertilization: D, H, L). Material was embedded in JB-4 resin, sectioned at 4 µm and stained for general structure (toluidine blue: A–D), cellulose and other polysaccharides (calcofluor white: E–H) or callose (aniline blue: I–L). The inner tangential wall of the nucellar epidermis did not stain strongly with toluidine blue throughout ovule development (A–D), but did stain strongly for cellulose, starting at the megaspore mother cell stage (E) with cell wall elaboration reaching a maximum by 0 d (G). After fertilization, cellulose was absent at the site of pollen tube penetration (arrowhead in H). Callose did not accumulate until -3 d (I), but subsequently formed a discrete layer just interior to the cellulosic wall convolutions of the inner tangential wall (J–K). This callose layer was not present after pollination (L). Scale bar = 10 µm.

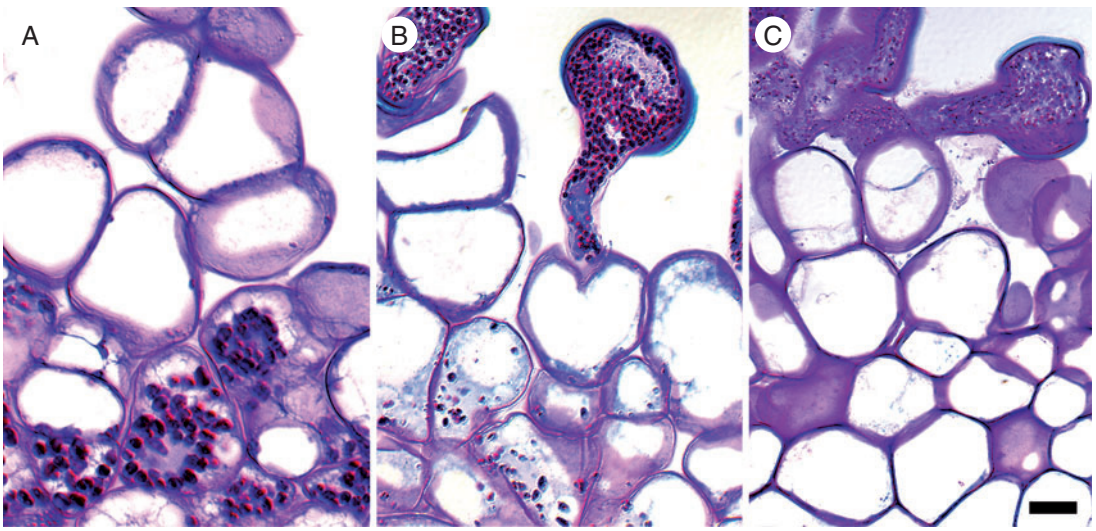

FIG. 4. Pollen–stigma interactions in *Nymphaea thermarum*. Material was embedded in JB-4 resin, sectioned at 4 µm and stained with PAS reagent and toluidine blue. (A) Starch presence in subdermal the stigmatoid layer, prior to pollination (-2 d). (B) Pollen grains with high starch content 1 d before anthesis (-1 d), with reduction in stigmatoid starch reserves. (C) Absence of starch in stigmatic tissue, second day of anthesis (1 d). Scale bar = 10 µm.

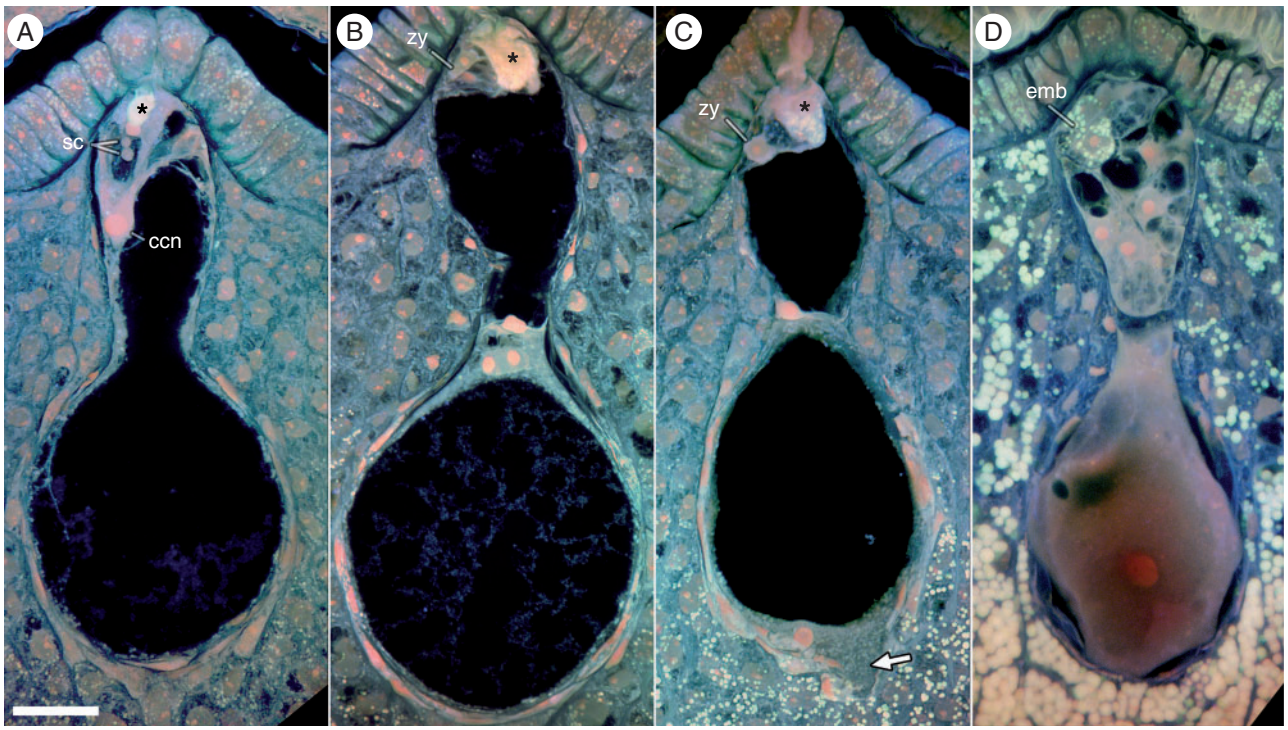

FIG. 5. Fertilization and endosperm differentiation in *Nymphaea thermarum*. Confocal images shown are maximum projections of ≥20 optical sections. Material was pretreated for the Feulgen reaction and embedded in JB-4 resin. (A) Pollen tube penetration of the nucellar cap and delivery of two sperm cells. The central cell nucleus is located next to the egg apparatus. (B) Primary endosperm nucleus migration and cellular division. Two endosperm domains are present: a micropylar endosperm domain and a chalazal endosperm domain. (C) Migration of chalazal endosperm domain nucleus to the chalazal pole and extension of a finger-like projection into the nucellus (arrow). The zygote and micropylar endosperm domain remain undivided. (D) The chalazal endosperm domain nucleus enlarges but does not divide. The micropylar endosperm domain has undergone several rounds of cell division, while the embryo is two-celled and has accumulated starch. Starch reserves are also present in the nucellus. The asterisk indicates pollen tube discharge. Abbreviations: ccn, central cell nucellus; emb, embryo; sc, sperm cells; zy, zygote. Scale bar = 10 μm.

accumulated starch, and the micropylar endosperm domain has undergone multiple rounds of cell division (Fig. 5D). The chalazal endosperm nucleus greatly increases in size, suggesting multiple rounds of endoreduplication. Starch content in the surrounding nucellar tissue dramatically increases. The formation of a cell wall during the primary endosperm division, as well as the subsequent creation of a multicellular micropylar domain and a unicellular chalazal domain, demonstrates that endosperm development in *N. thermarum* is *ab initio* cellular as well as highly bipolar.

Seed development

After fertilization, volumetric enlargement of the developing seed is accompanied by changes in the colour of the seed coat: fertilized ovules progress from colourless to bright red and then brown in mature seeds (Fig. 6, top row). At maturity (and until germination) a floating aril encompasses the micropylar half of the seed.

To examine the rate and pattern of volumetric enlargement of the embryo, endosperm and perisperm during seed maturation, whole seeds were evaluated with confocal imaging (Fig. 6, bottom row). Maternal tissue (perisperm and seed coat) accounts for the greatest proportion of seed volume throughout seed development. The micropylar endosperm domain reaches its maximum area by 8 d after anthesis. The outermost layer of the micropylar endosperm begins to differentiate at this time, with the rest of the micropylar endosperm cells becoming more vacuolate. The outer micropylar endosperm layer persists though seed maturity (around 22 d), while the rest of the space is eventually occupied by the expanding embryo. Eight or more days later (30 d), seed germination begins with the fracturing of the seed coat near the micropyle and subsequent emergence of the root apical meristem. Cotyledon expansion drives epicotyl emergence. The cotyledon tips remain in the seed and in direct contact with the single persistent layer of endosperm cells throughout germination.

While the micropylar endosperm persists and physically separates the embryo from direct contact with maternal tissues throughout seed maturation, the chalazal endosperm domain embarks on a distinct developmental trajectory (Fig. 7). Immediately after the first endosperm cell division that establishes the micropylar and chalazal domains, the chalazal domain/cell is larger than the micropylar domain (1 d) but undergoes a reduction in volume by 2 d after anthesis (2 d). Growth of the micropylar domain and shrinkage of the chalazal domain (4 d) continue until ∼8 d after anthesis, at which point the micropylar endosperm has expanded to its maximum volume (8 d). By seed maturity (20 d), the embryo has

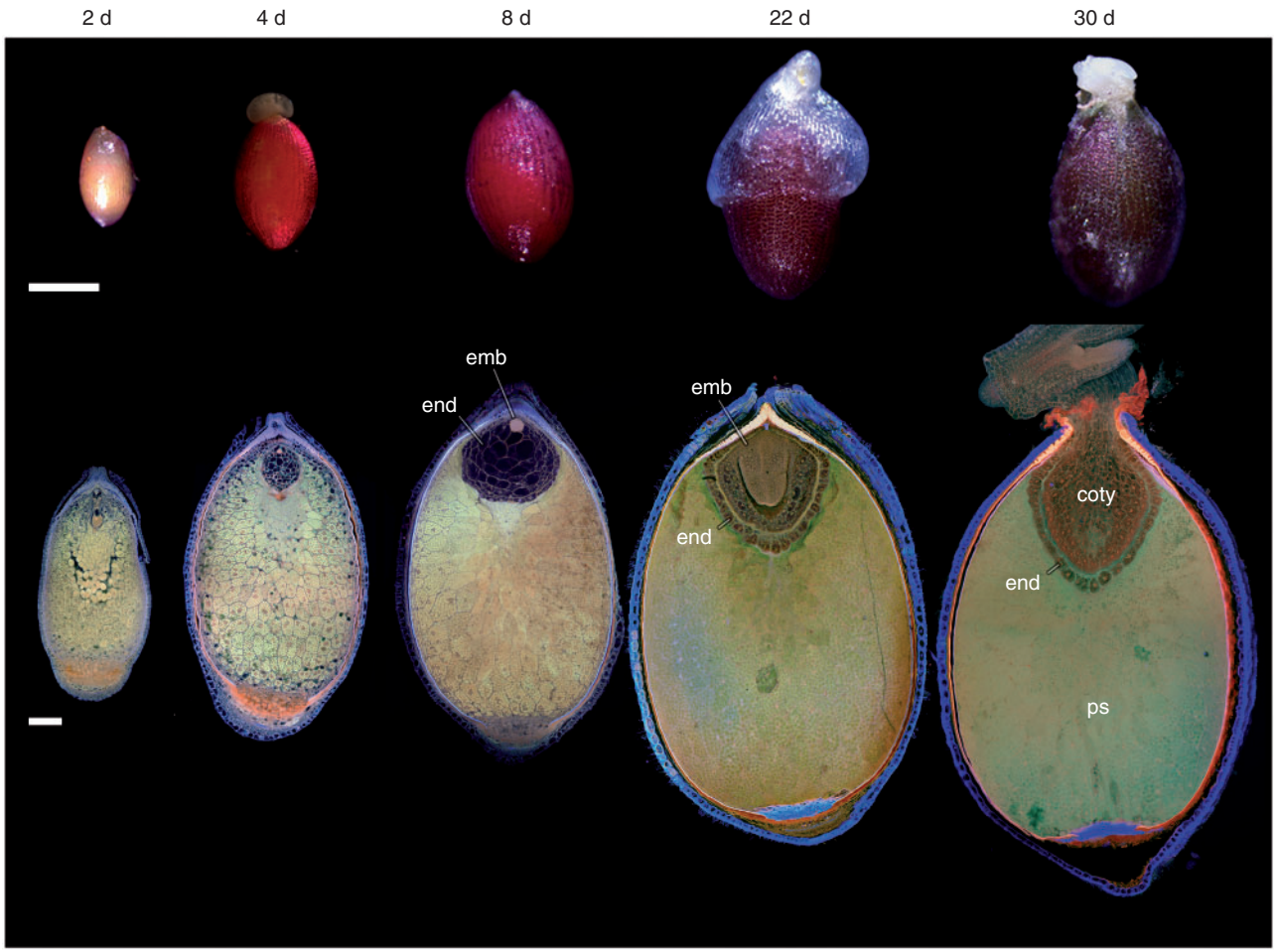

FIG. 6. Seed development in *Nymphaea thermarum*. Stereomicroscope images of seeds (top row) and single confocal optical sections or maximum projections of ≥20 optical sections; (bottom row) material treated for the Feulgen reaction. (Top row) External volumetric changes in developing seeds of *N. thermarum* accompanied a continued browning of the exotesta up to maturity (22 days after anthesis, noted as 22 d) and through germination (30 d). (Bottom row) Whole-mount imaging of seeds revealed that perisperm accounted for the majority of seed volume throughout development. The endosperm reached a maximum volume 8 d after anthesis (8 d). After this point, the growing embryo displaced most of the endosperm, leaving only the outermost layer of endosperm cells. This layer persisted through germination. Abbreviations: coty, cotyledons, end, endosperm; ps, perisperm. Scale bars = 100 μm.

undergone dramatic growth, mostly at the expense of the micropylar endosperm, and the chalazal domain is difficult to detect.

Insoluble polysaccharides during seed development

Reserves of insoluble polysaccharides accumulate in different offspring tissues at different times throughout development. Initially, all cells of the filamentous embryo contain starch (Fig. 8A), but these reserves become restricted to the suspensor with differentiation of the globular embryo proper (Fig. 8B) and subsequent initiation of the cotyledonary ridges by 8 d after fertilization (Fig. 8C). Starch grains are very rarely observed in the chalazal endosperm domain/cell (arrow) or the adjacent micropylar endosperm (Fig. 8D, E). However, beginning 8 d after fertilization, small aggregations of starch are present in the outermost layers of the micropylar endosperm (Fig. 8F).

Starch accumulates centrifugally in the perisperm immediately after fertilization, with the area adjacent to the chalazal endosperm domain acting as the focal point. Three perisperm zones are readily distinguished: the endosperm-adjacent zone, the transition zone and the peripheral zone. The endosperm-adjacent zone is an amorphous mass that is present throughout seed development (Fig. 8D–F). Distinct cells or cellular structures, such as nuclei and cell walls, are not evident. The transition zone is characterized by polygonal perisperm cells that transition from containing discrete starch aggregations and having identifiable nuclei (Fig. 8G) to being so full of starch that cellular structures become severely distorted (Fig. 8H, I). Finally, the peripheral zone is the outermost area of the perisperm, which is last to accumulate starch (Fig. 8J–L). Cells of the peripheral zone are elongated, rather than polygonal, and the accumulated aggregations of starch are smaller than those found elsewhere in the perisperm.

When the two cotyledons are initiated during embryo development (asterisks in Fig. 9A), the cells of the micropylar endosperm adjacent to the embryo become increasingly vacuolate and appear to degenerate. Starch density is reduced in the perisperm adjacent to the endosperm relative to its density in

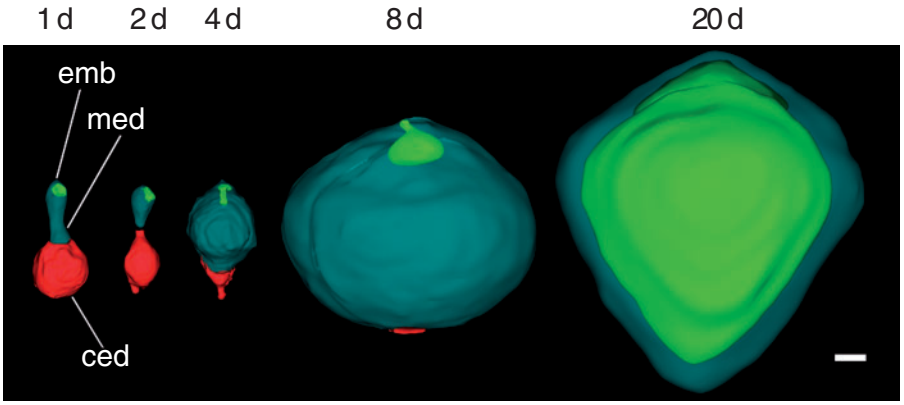

FIG. 7. Embryo–endosperm volumetric relationships in *Nymphaea thermarum*. Three-dimensional surface renderings of the developing offspring tissues reconstructed from z-stacks of whole-mount ovules. Offspring tissues are depicted on the second day of anthesis and at 2, 4, 8 and 20 days after anthesis (noted as 1 d, 2 d, 4 d, 8 d and 20 d, respectively). Immediately after fertilization, the chalazal endosperm domain was slightly larger than the micropylar domain. Growth of the micropylar domain occurred through 8 d, partly at the expense of the chalazal endosperm domain. The expansion of the embryo was comparatively negligible until after the micropylar endosperm reached its maximum volume. The chalazal domain was rarely evident after 8 d. By the time of seed maturity (20 d), the embryo had expanded into space previously occupied by the micropylar endosperm, displacing all but a single layer of peripheral endosperm cells. Abbreviations: ced, chalazal endosperm domain; emb, embryo; med, micropylar endosperm domain. Scale bar = 10 μm.

this zone at earlier stages. At seed maturity (20 d after anthesis), starch is present in the cotyledons of the expanded embryo and in the single layer of remaining endosperm (asterisks in Fig. 9B). The rest of the perisperm is completely full of starch, to the point of making individual cells difficult to distinguish, thus blurring the boundary between the endosperm-adjacent zone and the peripheral zone.

DISCUSSION

Flower and pollination biology of Nymphaea thermarum

The majority of extant basal angiosperm lineages with hermaphroditic flowers are protogynous (Thien *et al*., 2009; Endress, 2010). In most members of the Nymphaeaceae and Cabombaceae, protogyny is manifest as a discrete temporal separation between female and male phases, punctuated by the closing and reopening of the flower each day or night of anthesis (reviewed in Wiersema, 1988). In the day-blooming subgenus *Brachyceras* (of which *N. thermarum* is a member), this sequence occurs over ≥2 d: the flower opens on the first day as functionally female, with stigmatic secretion present and the stigmatic surface receptive, and then closes in the evening. The following morning, the flower reopens for ≥1 d as functionally male, as the anthers dehisce to disperse pollen (Heslop-Harrison, 1955*a*; Prance and Anderson, 1976; Wiersema, 1988; Orban and Bouharmont, 1995; Thien *et al*., 2009; Williams *et al*., 2010). Although flowers of *N. thermarum* open, close and reopen, as is typical for water lilies with separate female and male phases, they are incompletely protogynous. The overlap of female and male functions in *N. thermarum* is a consequence of the dehiscence of the outermost whorl(s) of anthers prior to anthesis, contemporaneously with the onset of stigmatic secretion. This advancement of male development relative to other floral ontogenetic events creates overlap between female and male functions. Furthermore, *N. thermarum* resembles other hermaphroditic members of Nymphaeales in that it is capable of self-pollination (Wiersema, 1988). Since pollen is released before the flower opens, and thus before the opportunity for the flower to receive outcrossing pollen, *N. thermarum* is not only capable of self-pollination, but is very likely predisposed to it.

Pollen release in bud has been described in three genera of Nymphaeaceae (Borsch *et al*., 2008): the monotypic genus *Euryale* (Okada and Otaya, 1930; Okada, 1938; Kadono and Schneider, 1987), *Barclaya* (Williamson and Schneider, 1994) and several species of *Nymphaea*, including *N. capensis* var. *zanzibarensis* (Prance and Anderson, 1976; Orban and Bouharmont, 1995), *N. ampla* (Prance and Anderson, 1976), *N. minuta* (Landon *et al*., 2007) and *N. thermarum*, as shown in the current work. The four *Nymphaea* species all belong to the tropical subgenus *Brachyceras* (Borsch *et al*., 2011), suggesting that acceleration of male development may be a trait that evolved in a common ancestor of this group. Overlap between female and male functions has been reported in other species of *Nymphaea* (*N. alba, N. amazonum*, *N. conardii*, *N. jamesoniana*, *N. ligulata* and *N. rudgeana*), but, in contrast to what we found in *N. thermarum*, can be due to late or prolonged female function rather than necessarily early male function (Wiersema, 1988). Assuming that protogyny is plesiomorphic for Nymphaeaceae, the partial breakdown of this dichogamous pattern appears to have evolved independently several times within the family, and can involve different heterochronic mechanisms that affect the relative timing of either or both female and male development events.

A biological predisposition towards self-pollination can have profound effects on population dynamics, and thus the evolutionary history of a species. On the one hand, self-compatibility can be advantageous in guaranteeing fruit production under unfavourable conditions, such as pollinator scarcity or in fragmented populations with few individuals in small patches (Pang and Saunders, 2014). Since *N. thermarum* is extinct in the wild, pollinator interactions are unknown, but populations were known to be fragmented (Fischer, 1988; Fischer and

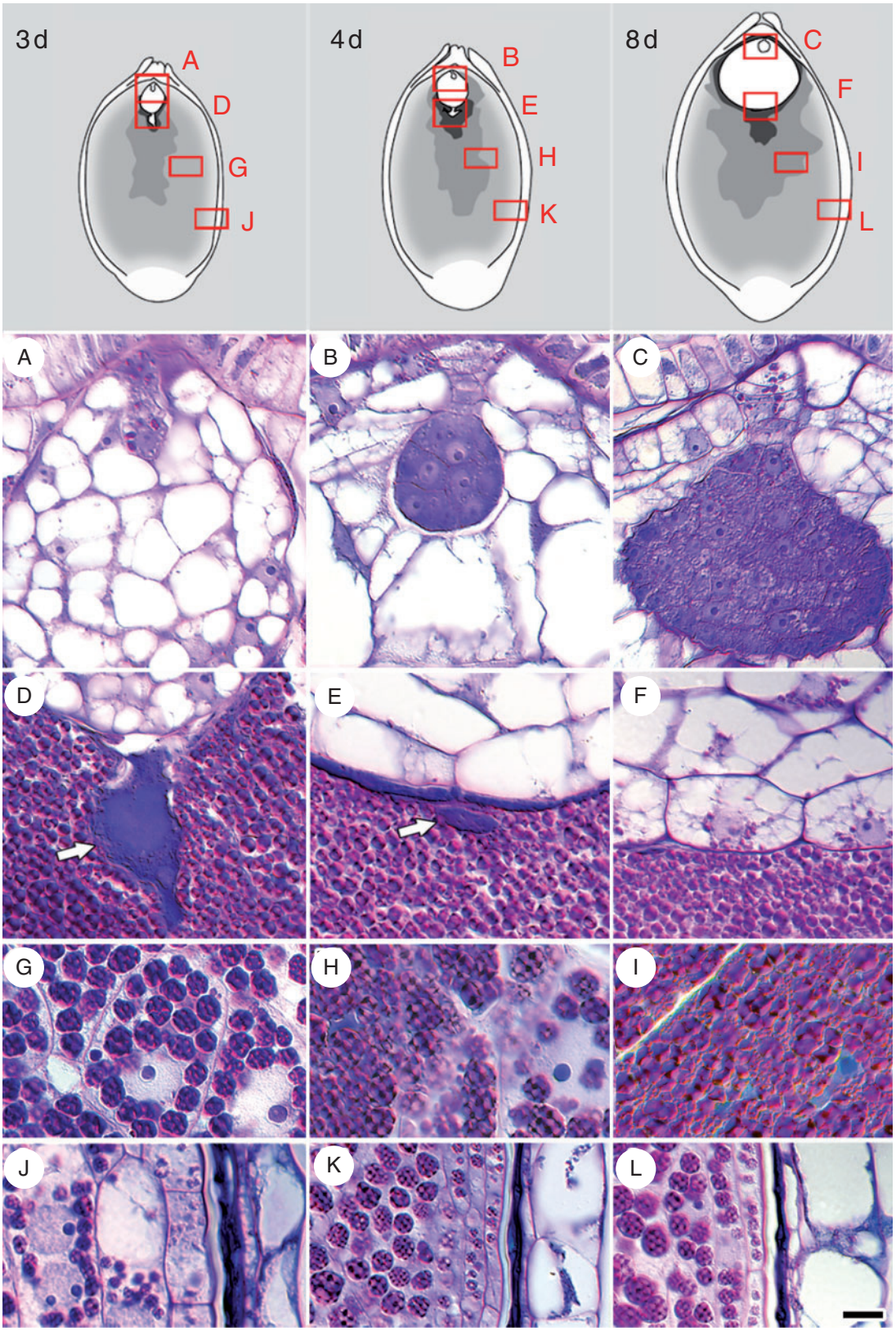

FIG. 8. Insoluble polysaccharide zonation in *Nymphaea thermarum* developing seeds. Material was embedded in JB-4 resin, sectioned at 4 µm and stained with PAS reagent and toluidine blue. Seeds were examined at 3 (A, D, G, J), 4 (B, E, H, K) and 8 days (C, F, I, L) after anthesis (noted as 3 d, 4 d and 8 d, respectively). (A) Initially, starch is present throughout the filamentous embryo, but is later restricted to the suspensor and nascent root pole in the late-globular embryo (B). (C) Inception of the cotyledonary ridges. (D) Early and dense accumulation of starch in the endosperm-adjacent zone of the perisperm. (D–F) Starch is consistently absent from the chalazal endosperm (arrow), but is present in the peripheral layers of the micropylar endosperm 8 d after anthesis. (G–I) Perisperm transition zone, in which cells progressively accumulate starch. (J) Perisperm peripheral zone with some multinucleate cells. (J–K) Starch accumulation is delayed relative to other perisperm zones. (L) Starch aggregations remain discrete, even 8 d after anthesis. Scale bar = 10 µm

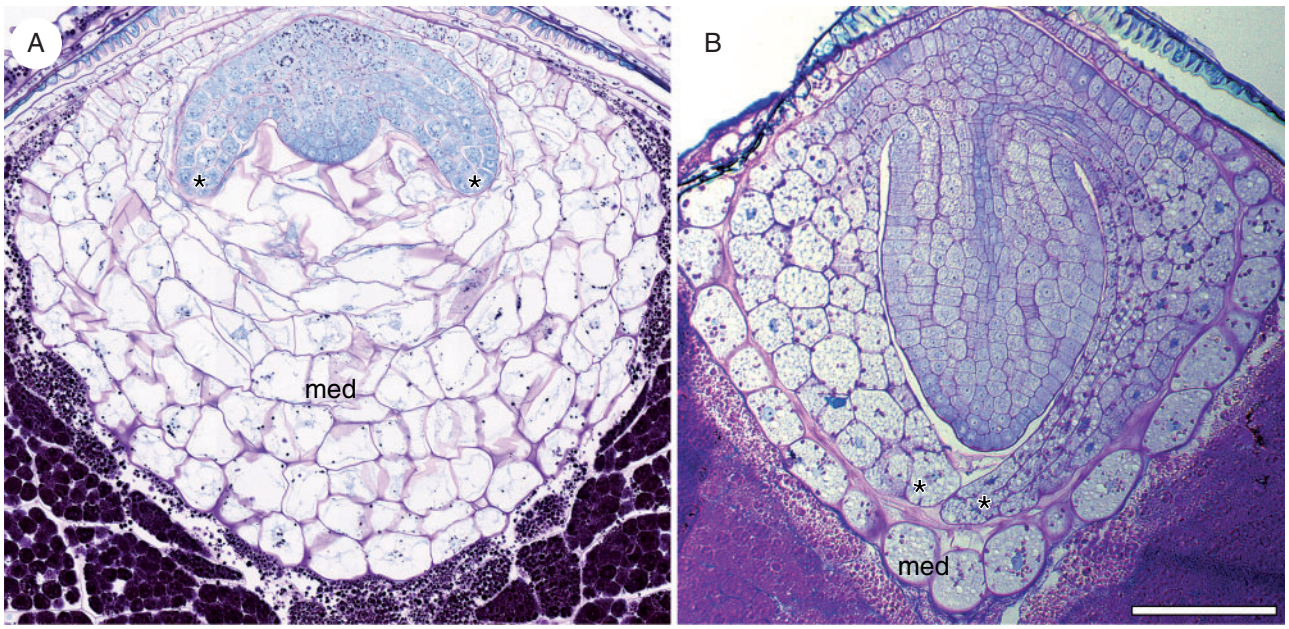

FIG. 9. Seed maturation in *Nymphaea thermarum*. Material was embedded in JB-4 resin, sectioned at 4 µm and stained with PAS reagent and toluidine blue. (A) Prior to seed maturation, two cotyledons (asterisks) are initiated. The cells of the micropylar endosperm near the embryo become increasing vacuolate and distorted as the cotyledons expand. Starch is present in the micropylar endosperm domain. (B) In mature seeds, the embryo has expanded, displacing the majority of the micropylar endosperm. Starch is present in the persistent endosperm and throughout the cotyledons (asterisks) of the embryo. Scale bar = 100 µm.

Magdalena-Rodriguez, 2010). On the other hand, widespread selfing may have actually played a role in the demise of the species. Generations of inbreeding can decrease the amount of genetic, and thus phenotypic, variation in small populations, leading to decreased times to population extinction (Brook *et al*., 2002; Frankham, 2005; Reed, 2005; Dornier and Cheptou, 2012). This effect, compounded by the fact that population size was already constrained by specialization for a limited habitat (hot springs), may have rendered *N. thermarum* unable to cope with rapid habitat loss. Understanding how the floral biology of *N. thermarum* may have factored into its near-extinction can help conservation efforts and prevent a similar fate for other tropical and non-tropical water lilies (Nierbauer *et al*., 2014). Other members of the subgenus *Brachyceras* that are similarly inclined towards self-pollination and found within limited ranges, such as the Madagascar-endemic *N. minuta* (Landon *et al*., 2007), are therefore of particular concern.

Ovule development in Nymphaea thermarum

Development of the female gametophyte and ovule of *N. thermarum* is generally in accordance with what is known from other members of the Nymphaeales. The female gametophyte of *N. thermarum* is of the *Nuphar*/*Schisandra* type, in that it is monosporic and four-nucleate, four-celled at maturity. This type of female gametophyte is characteristic of the most ancient flowering plant lineages described to date (Nymphaeales: Orban and Bouharmont, 1998; Williams and Friedman, 2002; Friedman, 2006, 2008; Rudall *et al*., 2008. Austrobaileyales: Friedman *et al*., 2003; Williams and Friedman, 2004; Tobe *et al*., 2007; Bachelier and Friedman, 2011), with the exception of *Amborella trichopoda*, which has a unique nine-nucleate, eight-celled female gametophyte (Friedman and Ryerson, 2009). Our observations of *N. thermarum* provide further support for the hypothesis that the *Nuphar*/*Schisandra*-type female gametophyte is the only type to be found among the Nymphaeales, despite decades of earlier reports that described the occurrence of the more complex and ubiquitous *Polygonum* type. These reports have been shown to almost certainly be erroneous (Williams and Friedman, 2002; Friedman and Williams, 2003).

During the free-nuclear stages of female gametophyte development in *N. thermarum*, simultaneous enlargement of the female gametophyte and degeneration of the micropylar nucellus puts the female gametophyte in direct contact with the single persistent layer of nucellar epidermis. The interior periclinal cell walls of this nucellar epidermal layer thicken and become convoluted in a manner reminiscent of transfer cell morphology. Similarly differentiated tissue in the micropylar part of the ovule has been referred to as epistase, but this phenomenon appears to be unusual and is poorly understood in terms of both development and function (Maheshwari, 1950). Wall thickening of the nucellar epidermis has been described in three additional species within *Nymphaea* (*N. advena*, *N. gigantea* and *N. odorata*) and in *Victoria amazonica* (Nymphaeaceae) (Cook, 1902, 1906; Winter and Sharmov, 1991), but was (likely mistakenly) attributed to sclerification. Cytological examination of *N. thermarum* reveals that these prominent convoluted cell walls are distinct from the filiform apparatus, and are composed of different layers of cellulose and callose that accumulate throughout ovule maturation.

Prolonged cellulose synthesis to create wall invaginations increases the surface area of the plasmalemma, and thus the capacity for solute transfer, and is a common feature of transfer

cell walls (Talbot *et al*., 2007). Callose is also associated with a number of transfer cell types: the gametophyte/sporophyte interface in mosses (Offler *et al*., 2003), nodules of legumes (Dahiya and Brewin, 2000) and endosperm tissue in cereal grains (Zheng and Wang, 2011; Thiel *et al*., 2012; Thiel, 2014). The dramatic disappearance of callose from this layer of nucellus upon pollen tube penetration in *N. thermarum* suggests that this layer might have a discrete function associated with pollen tube attraction, fertilization and/or early offspring growth. Our examination of the broader literature on angiosperm ovules indicates that this type of cell wall patterning in the nucellus adjacent to the egg apparatus (and separate from the filiform apparatus) is either unique to water lilies or significantly underreported (Maheshwari, 1950).

Seed ontogeny in Nymphaea thermarum

Studies of seed development in Nymphaeales are scattered across the last century of embryological research (Cook, 1902, 1906, 1909; Conard, 1905; Seaton, 1908; Martin, 1946; Meyer, 1960; Khanna, 1964*a*, *b*, 1965, 1967; Valtzeva and Savich, 1965; Schneider, 1978; Schneider and Ford, 1978; Batygina *et al*., 1980, 1982; Schneider and Jeter, 1982; Floyd and Friedman, 2000, 2001; Yamada *et al*., 2001; Williams and Friedman, 2002; Friedman, 2008; Friedman *et al*., 2012). Nevertheless, the more recent evaluations and reviews, which take advantage of taxonomic revisions, have revealed a number of common features of seed development in Nymphaeales: a perisperm (maternally derived storage tissue) that accounted for the majority of seed volume, a small diploid endosperm and a minute embryo.

Comparison of seed ontogenies among the three extant families of Nymphaeales (Hydatellaceae, Cabombaceae and Nymphaeaceae) indicates that details of endosperm development vary between, and even within, these families. Members of Hydatellaceae have a cellular endosperm that remains fairly undifferentiated (Rudall *et al*., 2009; Friedman *et al*., 2012). In Nymphaeaceae and Cabombaceae, division of the primary endosperm cell into two cells gives rise to a bipolar endosperm with two distinct domains: the micropylar domain, which surrounds the embryo, and the chalazal domain, which faces (and often penetrates) the maternal tissues of the perisperm (Cook, 1902, 1906, 1909; Seaton, 1908; Khanna, 1964*b*, 1965, 1967; Schneider and Jeter, 1982; Floyd and Friedman, 2000, 2001; Yamada *et al*., 2001). While the chalazal domain remains uninucleate, the divisions that take place in the micropylar domain can be either free nuclear (Cabombaceae) (Cook, 1906; Floyd and Friedman, 2000) or cellular (Nymphaeaceae) (Cook, 1902 1906, 1909; Seaton, 1908; Khanna, 1967; Schneider, 1978; Schneider and Ford, 1978; Floyd and Friedman, 2001) and will ultimately create the majority of endosperm tissue within the seed. The *ab initio* endosperm development in *N. thermarum* is fundamentally similar to what has been described in other members of the Nymphaeaceae.

Studies of seeds in *Nymphaea* typically have not recorded the complete ontogeny of the different tissues (Cook, 1902, 1906, 1909; Seaton, 1908; Khanna, 1964*a*, 1967; Batygina, 1980; Valtzeva and Savich, 1965; Rudall *et al*., 2009), and many have overlooked the development of the ephemeral chalazal endosperm domain. Our study of *N. thermarum* provides the most complete ontogeny of the chalazal endosperm domain in any species of *Nymphaea*. Notably, while the domain remains unicellular and uninucleate, it produces a single, minute projection that protrudes into the perisperm. The presence and extent of development of a chalazal endosperm protrusion varies across Nymphaeales (Fig. 10). In Hydatellaceae, the chalazal endosperm domain is not apparent and is in fact difficult to distinguish at all (Friedman *et al*., 2012). In Cabombaceae and *Nuphar* (Nymphaeaceae), the chalazal endosperm domain (protrusion) forms a large tube-like structure that penetrates the perisperm almost to the chalazal end of the seed, and persists at seed maturity (Cook, 1902, 1906, 1909; Seaton, 1908; Khanna, 1964*b*, 1965, 1967; Schneider and Jeter, 1982; Floyd and Friedman, 2000, 2001; Yamada *et al*., 2001).

The chalazal endosperm domain of several members of the Nymphaeales has been referred to as a haustorial structure, based primarily on its proximity to and apparent interaction with the perisperm tissue (Cook, 1902, 1906; Khanna, 1965, 1967; Valtzeva and Savich, 1965; Schneider and Jeter, 1982; Floyd and Friedman, 2000). We note that throughout Nymphaeales the degree of protrusion of the chalazal endosperm appears to correlate inversely with the presence of starch in the immediately adjacent perisperm at the time of chalazal endosperm development. Patterns of perisperm starch accumulation vary both spatially and temporally, and may contribute to variation in chalazal endosperm development. Before fertilization in Hydatellaceae, the entire perisperm is filled with starch (Friedman, 2008; Friedman *et al*., 2012). In Cabombaceae, post-fertilization starch accumulation in the perisperm is centripetal (Fig. 10). In *Nymphaea* (this study), starch first accumulates after fertilization at the centre of the perisperm and proceeds in a centrifugal pattern. While we cannot establish a causal link between centrifugal perisperm filling and 'stunted' chalazal endosperm development in *N. thermarum* compared with centripetal perisperm filling and prolonged chalazal development in *Cabomba*, our observations support the idea that chalazal endosperm development, and probably function, is intimately linked to nutrient dynamics within the seed.

Nymphaea thermarum *as a model system for illuminating early evolution of key angiosperm traits*

Extensive study of eudicot and monocot 'model' taxa has revealed much about the molecular biology and gene interactions that underlie flower and seed development (reviewed in e.g. Zanis, 2007; Litt and Kramer, 2010; Ruan *et al*., 2012; Dresselhaus and Doughty, 2014; Lafon-Placette and Köhler, 2014; Ó'Maoiléidigh *et al*., 2014). However, we know relatively little about how these processes operate in early-diverging angiosperm lineages (Soltis *et al*., 2007; Chanderbali *et al*., 2010). Consequently, it has not been possible to reconstruct the molecular development of flowers and reproductive processes during the earliest phases of angiosperm evolution.

The lack of genetic and molecular studies in the most ancient angiosperm lineages is not without good reason: the majority of taxa in these clades are woody and long-lived, which makes them unsuitable as subjects for molecular and genetic experiments. During the last 5 years, three herbaceous members of

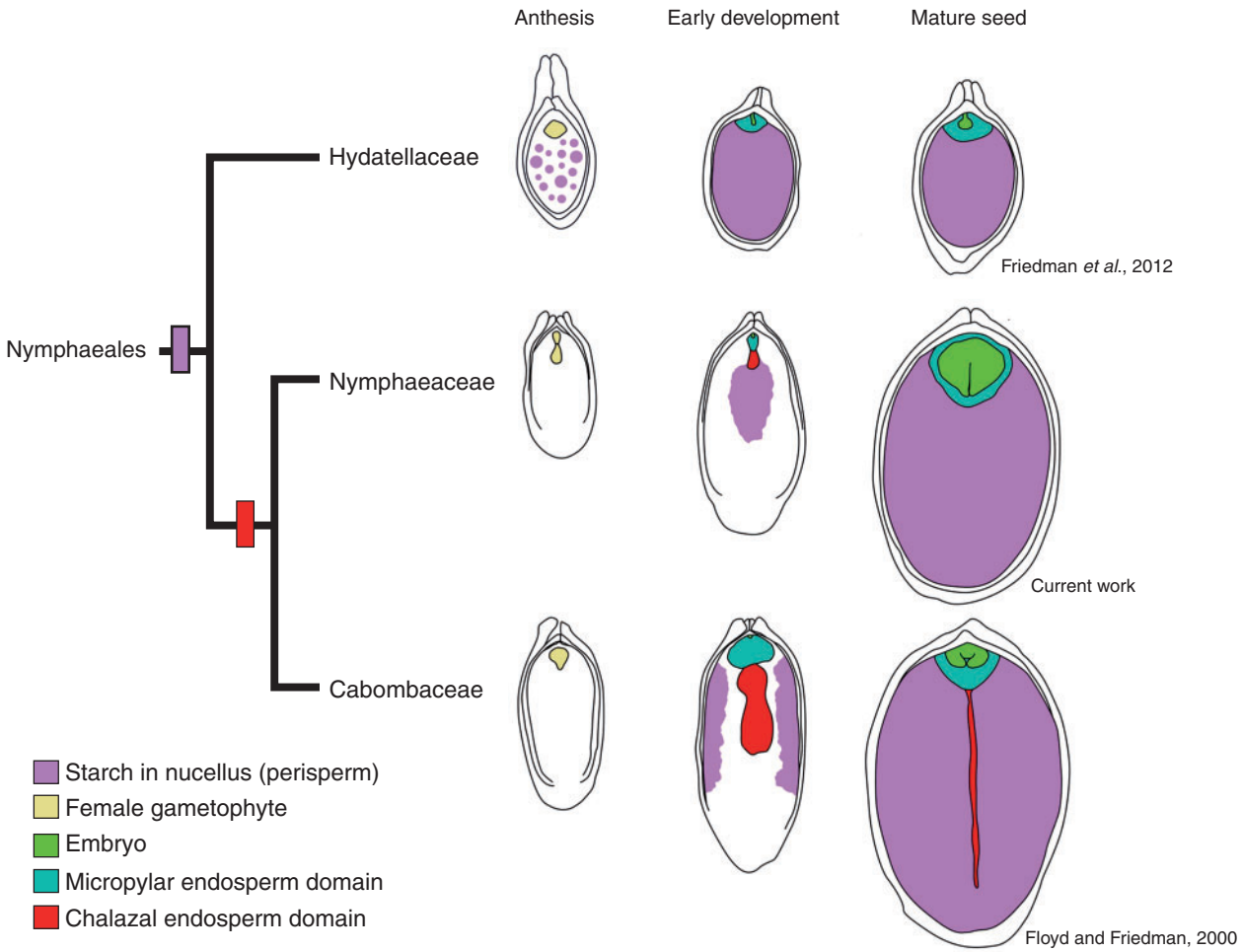

FIG. 10. Patterns of starch accumulation in the maternal tissues during seed development of Nymphaeales. While members of the Hydatellaceae show starch accumulation (pink) throughout the perisperm before fertilization, in *Nymphaea* (Nymphaeaceae) starch accumulates centrifugally in the perisperm after fertilization, and the chalazal endosperm (red) is ephemeral. In turn, *Cabomba* (Cabombaceae) shows centripetal starch accumulation in the perisperm, and the chalazal endosperm protrudes into the perisperm and persists at seed maturity. Teal, micropylar endosperm domain; green, embryo; beige, female gametophyte.

basal angiosperm lineages have been suggested as possible model systems: *Trithuria* (Hydatellaceae) (Rudall *et al.*, 2009), *Cabomba caroliniana* (Cabombaceae) (Vialette-Guiraud *et al.*, 2011) and *Aristolochia fimbriata* (Aristolochiaceae, Piperales) (Bliss *et al.*, 2013). As of now, none of these taxa has been embraced as a major model system. We suggest that *N. thermarum* has a unique potential for development into a model system. Many of its growth requirements have already been established (Fischer and Magdalena Rodriguez, 2010). The diminutive size of *N. thermarum* means that large numbers of individuals can be maintained in greenhouses or growth chambers, and although they are 'aquatic' these plants can be raised in individual pots placed in shallow tanks or tubs. Importantly, *N. thermarum* has a short life cycle of 5–6 months from seed germination to seed production, a generational timeframe that is exceedingly rare among basal angiosperms. Each flower can produce hundreds of seeds following either self-pollination or, if the maternal flower is emasculated at least one full day before anthesis, cross-pollination. A small genome size ($1C = 0{\cdot}51$ pg, only about twice the size of that of *A. thaliana*) further makes this system tractable for genetic experimentation (Pellicer *et al.*, 2013). Indeed, work is under way to produce transcriptomes from a variety of tissues, generate isogenic lines and develop stable transformation protocols. An annotated genome would complete the package of creating a model system taxon rooted deeply at the base of flowering plant phylogeny.

Finally, the results from this study establish a timeline for female reproductive development, floral biology and seed development. A firm understanding of the reproductive biology of *N. thermarum*, combined with information on remaining genetic diversity maintained in *ex situ* collections, will be essential for any attempt to reintroduce populations into the wild and conserve this remarkable species.

ACKNOWLEDGEMENTS

We thank Ekaterina Morozova for help with sectioning and the staff of Botanische Gärten der Universität Bonn for providing plant material for propagation. This work was

supported by a grant from the National Science Foundation (grant number IOS-S-0919986) to W.E.F.

LITERATURE CITED

Bachelier JB, Friedman WE. 2011. Female gamete competition in an ancient angiosperm lineage. *Proceedings of the National Academy of Sciences of the USA* **180**: 12360–12365.

Baker HG, Baker I. 1979. Starch in angiosperm pollen grains and its evolutionary significance. *American Journal of Botany* **66**: 591–600.

Barrell P, Grossniklaus U. 2005. Confocal microscopy of whole ovules for analysis of reproductive development: the *elongate1* mutant affects meiosis II. *Plant Journal* **43**: 309–320.

Baskin CC, Baskin JM. 2007. Nymphaeaceae: a basal angiosperm family (ANITA grade) with a fully developed embryo. *Seed Science Research* **17**: 293–296.

Batygina TB, Kravtsova TI, Shamrov II. 1980. The comparative embryology of some representatives of the orders Nymphaeales and Nelumbonales. *Botanicheskii Zhurnal* **65**: 1071–1086.

Batygina TB, Shamrov II, Kolesova GE. 1982. Embryology of the Nymphaeales and Nelumbonales II. The development of the female embryonic structures. *Botanicheskii Zhurnal* **67**: 117S–119S.

Bliss BJ, Wanke S, Barakat A, *et al.* 2013. Characterization of the basal angiosperm *Aristolochia fimbriata*: a potential experimental system for genetic studies. *BMC Plant Biology* **13**: 13. doi:10.1186/1471-2229-13-13.

Bonilla-Barbosa J, Novelo A, Orozco YH, Márquez-Guzmán J. 2000. Comparative seed morphology of Mexican *Nymphaea* species. *Aquatic Botany* **68**: 189–204.

Borsch T, Löhne C, Mbaye MS, Wiersema J. 2011. Towards a complete species tree of *Nymphaea*: shedding further light on subg. *Brachyceras* and its relationship to the Australian water-lilies. *Telopea* **13**: 193–217.

Borsch T, Löhne C, Wiersema J. 2008. Phylogeny and evolutionary patterns in Nymphaeales: integrating genes, genomes and morphology. *Taxon* **57**: 1052–1081.

Brook BW, Tonkyn DW, Q'Grady JJ, Frankham R. 2002. Contribution of inbreeding depression to extinction risk in threatened species. *Conservation Ecology* **6**: 16.

Čapek M, Janáček J, Kubìnová L. 2006. Methods of compensation of the light attenuation with depth of images captured by a confocal microscope. *Microscopy Research and Technique* **69**: 624–635.

Capperino ME, Schneider EL. 1985. Floral biology of *Nymphaea mexicana* Zucc. (Nymphaeaceae). *Aquatic Botany* **23**: 83–93.

Chanderbali AS, Yoo M, Zahn LM, *et al.* 2010. Conservation and canalization of gene expression during angiosperm diversification accompany the origin and evolution of the flower. *Proceedings of the National Academy of Sciences of the USA* **107**: 22570–22575.

Chiflot JBJ. 1902. Contributions a l'etude de la classe des Nympheinees. *Annales de l'Université de Lyon, nouvelle série*. **10**: 1–294.

Conard HS. 1905. *The water lilies: a monograph of the genus Nymphaea*. Washington: Carnegie Institution of Washington.

Cook MT. 1902. Development of the embryo-sac and embryo of *Castalia odorata* and *Nymphaea advena*. *Bulletin of the Torrey Botanical Club* **29**: 211–220.

Cook MT. 1906. The embryogeny of some Cuban Nymphaeaceae. *Botanical Gazette* **42**: 376–392.

Cook MT. 1909. Notes on the embryology of Nymphaeaceae. *Botanical Gazette* **48**: 56–59.

Currier HB. 1957. Callose substance in plant cells. *American Journal of Botany* **44**: 478–488.

Dahiya P, Brewin NJ. 2000. Immunogold localization of callose and other cell wall components in pea nodule transfer cells. *Protoplasma* **214**: 210–218.

Dornier A, Cheptou P. 2012. Determinants of extinction in fragmented plant populations: *Crepis sancta* (Asteraceae) in urban environments. *Oecologia* **169**: 703–712.

Doyle JA, Endress PK. 2014. Integrating early Cretaceous fossils into the phylogeny of living angiosperms: ANITA lines and relatives of Chloranthaceae. *International Journal of Plant Sciences* **175**: 555–600.

Dresselhaus T, Doughty J. 2014. Regulation of fertilization and early seed development. *Biochemical Society Transactions* **42**: 309–312.

Endress PK. 2001. The flowers in extant basal angiosperms and inferences on ancestral flowers. *International Journal of Plant Sciences* **162**: 1111–1140.

Endress PK. 2005. Carpels in *Brasenia* (Cabombaceae) are completely ascidiate despite a long stigmatic crest. *Annals of Botany* **96**: 209–215.

Endress PK. 2010. The evolution of floral biology in basal angiosperms. *Philosophical Transactions of the Royal Society, B. Biological Sciences* **365**: 411–421.

Feder N, O'Brien TP. 1968. Plant microtechnique: some principles and new methods. *American Journal of Botany* **55**: 123–142.

Fischer E. 1988. Beiträge zur Flora Zentralafrikas I. Eine neue *Nymphaea* sowie ein neuer *Streptocarpus* aus Rwanda. *Feddes Repertorium* **99**: 385–390.

Fischer E, Magdalena-Rodriguez C. 2010. *Nymphaea thermarum* (Nymphaeaceae). *Curtis Botanical Magazine* **27**: 318–327.

Floyd SK, Friedman WE. 2000. Evolution of endosperm developmental patterns among basal flowering plants. *International Journal of Plant Sciences* **16**: S57–S81.

Floyd SK, Friedman WE. 2001. Developmental evolution of endosperm in basal angiosperms: evidence from *Amborella* (Amborellaceae), *Nuphar* (Nymphaeaceae), and *Illicium* (Illiciaceae). *Plant Systematics and Evolution* **228**: 153–169.

Frankham R. 2005. Genetics and extinction. *Biological Conservation* **126**: 131–140.

Friedman WE. 2006. Embryological evidence for developmental lability during early angiosperm evolution. *Nature* **441**: 337–340.

Friedman WE. 2008. Hydatellaceae are water lilies with gymnospermous tendencies. *Nature* **453**: 94–97.

Friedman WE, Ryerson KC. 2009. Reconstructing the ancient female gametophyte in angiosperms: insights from *Amborella* and other ancient lineages of flowering plants. *American Journal of Botany* **96**: 129–143.

Friedman WE, Williams JH. 2003. Modularity of the angiosperm female gametophyte and its bearing on the early evolution of endosperm in flowering plants. *Evolution* **57**: 216–230.

Friedman WE, Gallup WN, Williams JH. 2003. Gametophyte development in *Kadsura*: implications for Schisandraceae, Austrobaileyales, and the early evolution of flowering plants. *International Journal of Plant Sciences* **164**: S293–S305.

Friedman WE, Bachelier JB, Hormaza JI. 2012. Embryology in *Trithuria submersa* (Hydatellaceae) and relationships between embryo, endosperm, and perisperm in early-diverging flowering plants. *American Journal of Botany* **99**: 1083–1095.

Friis EM, Pedersen KR, Crane, PR. 2001. Fossil evidence of water lilies (Nymphaeales) in the early Cretaceous. *Nature* **410**: 357–360.

Friis EM, Pedersen KR, Crane PR. 2006. Cretaceous angiosperm flowers: innovation and evolution in plant reproduction. *Palaeo* **232**: 251–293.

Friis EM, Crane PR, Pedersen KR. 2011. *Early flowers and angiosperm evolution*. Cambridge: Cambridge University Press.

Grob V, Moline P, Pfeifer E, Novelo AR, Rutishauser R. 2006. Developmental morphology of branching flowers in *Nymphaea prolifera*. *Journal of Plant Research* **119**: 561–570.

Heslop-Harrison Y. 1955*a*. Biological flora of the British Isles. *Nuphar* Sm. *Journal of Ecology* **43**: 342–364.

Heslop-Harrison Y. 1955*b*. Biological flora of the British Isles. *Journal of Ecology* **43**: 719–734.

Hu GW, Lei LG, Liu KM, Long CL. 2009. Floral development in *Nymphaea tetragona* (Nymphaeaceae). *Botanical Journal of the Linnean Society* **159**: 211–221.

Hughes J, McCully ME. 1975. The use of an optical brightener in the study of plant structure. *Stain Technology* **50**: 319–329.

Iles WD, Lee C, Sokoloff DD, *et al.* 2014. Reconstructing the age and historical biogeography of the ancient flowering-plant family Hydatellaceae (Nymphaeales). *BMC Evolutionary Biology* **14**: 120. doi:10.1186/1471-2148-14-102.

Kadono Y, Schneider EL. 1987. The life history of *Euryale ferox* Salisb. in southwestern Japan with special reference to reproductive ecology. *Plant Species Biology* **2**: 109–115.

Khanna P. 1964a. Some interesting observations in *Euryale ferox* Salisb. *Current Science* **33**: 152.

Khanna P. 1964b. Morphological and embryological studies in Nymphaeaceae. I. *Euryale ferox* Salisb. *Proceedings of the Indian Academy of Sciences* **59**: 237–244.

Khanna P. 1965. Morphological and embryological studies in Nymphaeaceae. II. *Brasenia schreberi* Gmel. and *Nelumbo nucifera* Gaertin. *Australian Journal of Botany* **13**: 379–387.

Khanna P. 1967. Morphological and embryological studies in Nymphaeaceae III. *Victoria cruziana* D'Orb., and *Nymphaea stellate* Willd. *Botanical Magazine Tokyo* **80**: 305–312.

Lafon-Placette C, Köhler C. 2014. Embryo and endosperm, partners in seed development. *Current Opinion in Plant Biology* **17**: 64–69.

Landon K, Nozaic PI, Edwards RA. 2007. A new species of water lily (*Nymphaea minuta*: Nymphaeaceae) from Madagascar. *Water Garden Journal* **22**: 5–10.

Litt A, Kramer, EM. 2010. The ABC model and the diversification of floral organ identity. *Seminars in Cell & Developmental Biology* **21**: 129–137.

Magallón S, Hilu KW, Quandt D. 2013. Land plant evolutionary timeline: gene effects are secondary to fossil constraints in relaxed clock estimation of age and substitution rates. *American Journal of Botany* **100**: 556–573.

Maheshwari P. 1950. *An introduction to the embryology of angiosperms*. New York: McGraw Hill.

Maia VH, Gitzendanner MA, Soltis PA, Wong GK, Soltis DE. 2014. Angiosperm phylogeny based on 18S/26S rDNA sequence data: constructing a large data set using next-generation sequence data. *International Journal of Plant Sciences* **75**: 613–650.

Martin AC. 1946. The comparative internal morphology of seeds. *American Midland Naturalist* **36**: 513–660.

Meyer KI. 1960. On the embryology of *Nuphar luteum* Sm. *Bulletin of Moscow Society of Naturalists, Biological Series* **65**: 48–60.

Van Miegroet F, Dujardin M. 1992. Cytologie et histologie de la reproduction chez le *Nymphaea heudelotii*. *Canadian Journal of Botany* **70**: 1991–1996.

Moseley MF. 1961. Morphological studies of the Nymphaeaceae II. The flower of *Nymphaea*. *Botanical Gazette* **122**: 233–259.

Moseley MF, Mehta IJ, Williamson PS, Kosakai H. 1984. Morphological studies of the Nymphaeaceae (sensu lato). XIII. Contributions to the vegetative and floral structure of *Cabomba*. *American Journal of Botany* **71**: 902–924.

Nierbauer KU, Kanz B, Zizka G. 2014. The widespread naturalization of *Nymphaea* hybrids is masking the decline of wild-type *Nymphaea alba* in Hesse, Germany. *Flora* **209**: 122–130.

Ó'Maoiléidigh DS, Graciet E, Wellmer F. 2014. Gene networks controlling *Arabidopsis thaliana* flower development. *New Phytologist* **201**: 16–30.

Offler CE, McCurdy DW, Patrick JW, Talbot MJ. 2003. Transfer cells: cells specialized for a special purpose. *Annual Review of Plant Biology* **54**: 431–454.

Okada, Y. 1938. On chasmogamous flowers of *Euryale ferox* Salisb. *Ecological Reviews* **4**: 159–163 (in Japanese).

Okada Y, Otaya T. 1930. Study of *Euryale ferox* Salisb. VI. Cleistogamous versus chasmogamous flower. *Botanical Magazine Tokyo* **44**: 369–373.

Orban I, Bouharmont J. 1995. Reproductive biology of *Nymphaea capensis* Thunb. var. *zanzibariensis* (Casp.) Verdc. (Nymphaeaceae). *Botanical Journal of the Linnean Society* **119**: 35–43.

Orban I, Bouharmont J. 1998. Megagametophyte development of *Nymphaea nouchali* Burm. F. (Nymphaeaceae). *Botanical Journal of the Linnean Society* **126**: 339–348.

Pang C, Saunders RMK. 2014. The evolution of alternative mechanisms that promote outcrossing in Annonaceae, a self-compatible family of early-divergent angiosperms. *Botanical Journal of the Linnean Society* **174**: 93–109.

Pellicer J, Kelly LJ, Magdalena C, Leitch IJ. 2013. Insights into the dynamics of genome size and chromosome evolution in the early diverging angiosperm lineage Nymphaeales (water lilies). *Genome* **56**: 1–13.

Prance GT, Anderson AB. 1976. Studies of the floral biology of tropical Nymphaeaceae. *Acta Amazonica* **6**: 163–170.

Qiu YL, Lee J, Bernasconi-Quadroni F, *et al.* 1999. The earliest angiosperms: evidence from mitochondrial, plastid and nuclear genomes. *Nature* **402**: 404–407.

Ramji MV, Padmanabhan D. 1965. Developmental studies on *Cabomba caroliniana* Gray I. Ovule and carpel. *Proceedings of the Indian Academy of Sciences Section B* **62**: 215–223.

Reed DH. 2005. Relationship between population size and fitness. *Conservation Biology* **19**: 563–568.

Ruan Y, Patrick JW, Bouzayen M, Fernie AR. 2012. Molecular regulation of seed and fruit set. *Trends in Plant Science* **17**: 656–665.

Rudall PJ, Sarkoloff DD, Remizowa MV, *et al.* 2007. Morphology of Hydatellaceae, an anomalous aquatic family recently recognized as an early-divergent angiosperm lineage. *American Journal of Botany* **94**: 1073–1092.

Rudall PJ, Remizowa MV, Beer AS, *et al.* 2008. Comparative ovule and megagametophyte development in Hydatellaceae and water lilies reveal a mosaic of features among the earliest angiosperms. *Annals of Botany* **101**: 941–956.

Rudall PJ, Eldridge T, Tratt J *et al.* 2009. Seed fertilization, development, and germination in Hydatellaceae (Nymphaeales): implications for endosperm evolution in early angiosperms. *American Journal of Botany* **96**: 1581–1593.

Ruhfel BR, Gitzendanner MA, Soltis PS, Soltis DE, Burleigh JG. 2014. From algae to angiosperms—inferring the phylogeny of green plants (Viridiplantae) from 360 plastid genomes. *BMC Evolutionary Biology* **14**: 23.

Saarela JM, Rai HS, Doyle JA, *et al.* 2007. Hydatellaceae identified as a new branch near the base of the angiosperm phylogenetic tree. *Nature* **446**: 312–315.

Schneider EL. 1976. The floral anatomy of *Victoria* Schomb. (Nymphaeaceae). *Botanical Journal of the Linnean Society* **72**: 115–148.

Schneider EL. 1978. Morphological studies of the Nymphaeaceae IX. The seed of *Barclaya longifolia* Wall. *Botanical Gazette* **139**: 223–230.

Schneider, EL. 1982. Observations on the pollination biology of *Nymphaea gigantea* WJ Hooker (Nymphaeaceae). *Western Australian Naturalist* **15**: 71–72.

Schneider EL. 1983. Gross morphology and floral biology of *Ondinea purpurea* den Hartog. *Australian Journal of Botany* **31**: 371–382.

Schneider EL, Chaney T. 1981. The floral biology of *Nymphaea odorata* (Nymphaeaceae). *Southwestern Naturalist* **26**: 159–165.

Schneider EL, Ford EG. 1978. Morphological studies of the Nymphaeaceae. X. The seed of *Ondinea purpurea* Den Hartog. *Bulletin of the Torrey Botanical Club* **105**: 192–200.

Schneider EL, Jeter JM. 1982. Morphological studies of the Nymphaeaceae XII. The floral biology of *Cabomba caroliniana*. *American Journal of Botany* **69**: 1410–1419.

Schneider EL, Moore LA. 1977. Morphological studies of the Nymphaeaceae. VII. The floral biology of *Nuphar lutea* subsp. macrophylla. Brittonia **29**: 88–99.

Schneider EL, Tucker SC, Williamson PS. 2003. Floral development in the Nymphaeales. *International Journal of Plant Sciences* **164**: S279–S292.

Seaton S. 1908. The development of the embryo-sac of *Nymphaea advena*. *Bulletin of the Torrey Botanical Club* **35**: 283–290.

Sokoloff DD, Remizowa MV, Briggs BG, *et al.* 2009. Shoot architecture and branching pattern in perennial Hydatellaceae (Nymphaeales). *International Journal of Plant Sciences* **170**: 869–884.

Sokoloff DD, Remizowa MV, Yadav SR, *et al.* 2010. Development of reproductive structures in the sole Indian species of Hydatellaceae, *Trithuria konkanensis*, and its morphological differences from Australian taxa. *Australian Systematic Botany* **23**: 217–228.

Soltis DE, Chanderbali AS, Kim S, Buzgo M, Soltis PS. 2007. The ABC model and its applicability to basal angiosperms. *Annals of Botany* **100**: 155–163.

Stevens PF. 2001. *Angiosperm phylogeny website*. http://www.mobot.org/MOBOT/research/APweb/.

Talbot MJ, Wasteneys GO, Offler CE, McCurdy DW. 2007. Cellulose synthesis is required for deposition of reticulate wall ingrowths in transfer cells. *Plant Cell Physiology* **48**: 147–158.

Thiel J, Riewe D, Rutten T, *et al.* 2012. Differentiation of endosperm transfer cells of barley: a comprehensive analysis at the micro-scale. *Plant Journal* **71**: 639–655.

Thiel J. 2014. Development of endosperm transfer cells in barley. *Frontiers in Plant Science* **5**: 108. doi: 10.3389/fpls.2014.00108.

Thien LB, Bernhardt P, Devall MS, *et al.* 2009. Pollination biology of basal angiosperms (ANITA grade). *American Journal of Botany* **96**: 166–182.

Tobe H, Kimoto Y, Prakash N. 2007. Development and structure of the female gametophyte in *Austrobaileya scandens* (Austrobaileyaceae). *Journal of Plant Research* **120**: 431–436.

Valtzeva OV, Savich EI. 1965. Development of embryo in *Nymphaea candida* Presl. and *N. tetragona* Georgi. *Botanicheskii Zhurnal* **50**: 1323–1326.

Vialette-Guiraud ACM, Alaux M, Legeai F, *et al.* 2011. *Cabomba* as a model for studies of early angiosperm evolution. *Annals of Botany* **108**: 589–598.

Wiersema JH. 1988. Reproductive biology of *Nymphaea* (Nymphaeaceae). *Annals of the Missouri Botanical Garden* **75**: 795–804.

Williams JH, Friedman WE. 2002. Identification of diploid endosperm in an early angiosperm lineage. *Nature* **415**: 522–526.

Williams JH, Friedman WE. 2004. The four-celled female gametophyte of Illicium (Illiciaceae; Austrobaileyales): implications for understanding the origin and early evolution of monocots, eumagnoliids, and eudicots. *American Journal of Botany* **91**: 332–357.

Williams JH, McNeilage RT, Lettre MT, *et al.* 2010. Pollen tube growth and the pollen-tube pathway of *Nymphaea odorata* (Nymphaeaceae). *Botanical Journal of the Linnean Society* **162**: 581–593.

Williamson PS, Moseley MF. 1989. Morphological studies of the Nymphaeaceae sensu lato. XVII. Floral anatomy of *Ondinea purpurea* subspecies *Purpurea* (Nymphaeaceae). *American Journal of Botany* **76**: 1779–1794.

Williamson PS, Schneider EL. 1994. Floral aspects of *Barclaya* (Nymphaeaceae): pollination, ontogeny and structure. *Plant Systematics and Evolution* **8**: 159–173.

Winter AN, Shamrov II. 1991. Megasporogenesis and embryo sac development in representatives of the genera *Nymphaea* and *Victoria* (Nymphaeaceae). *Botanicheskii Zhurnal* **76**: 1716–1728.

Yamada T, Imaichi R, Kato, M. 2001. Developmental morphology of ovules and seeds of Nymphaeales. *American Journal of Botany* **88**: 963–974.

Zanis MJ. 2007. Grass spikelet genetics and duplicate gene comparisons. *International Journal of Plant Sciences* **168**: 93–110.

Zheng Y, Wang Z. 2011. Contrast observation and investigation of wheat endosperm transfer cells and nucellar projection transfer cells. *Plant Cell Reports* **30**: 1281–1288.

Zhou Q, Fu D. 2007. Floral biology of *Nuphar pumila* (Timm) DC. (Nymphaeaceae) in China. *Plant Systematics and Evolution* **264**: 101–108.

Zhou Q, Fu D. 2008. Reproductive morphology of *Nuphar* (Nymphaeaceae), a member of basal angiosperms. *Plant Systematics and Evolution* **272**: 79–96.